

Synthesis of magnetic graphene composites for preconcentration trace amounts of malachite green and crystal violet from water

Yaping Zhong¹, Xue Wang¹, Yu He^{1,2}, Yili Ge^{1,2}, Gongwu Song^{1,2}

¹Ministry of Education Key Laboratory for the Synthesis and Application of Organic Functional Molecules, College of Chemistry and Chemical Engineering, Hubei University, Wuhan 430062, People's Republic of China

²Hubei Collaborative Innovation Center for Advanced Organic Chemical Materials, College of Chemistry and Chemical Engineering, Hubei University, Wuhan 430062, People's Republic of China

E-mail: heyu@hubei.edu.cn

Published in Micro & Nano Letters; Received on 2nd April 2015; Accepted on 15th June 2015

Graphene/silica magnetic nanocomposites are synthesised and introduced as new and reusable adsorbents for rapid and high-efficiency preconcentration trace amounts of dye pollutants in water. This method is simple, fast, cheap and non-toxic. The optimum adsorption conditions for the preconcentration of crystal violet (CV) and malachite green (MG) are investigated and the adsorption mechanisms are also discussed. The regeneration and reuse experiments showed the good reusability of the as-prepared adsorbent. In addition, this method was successfully applied to the preconcentration of trace amounts of MG and CV from water samples, which presages more opportunities for application in environmental and material sciences.

1. Introduction: Crystal violet (CV) and malachite green (MG), both triphenylmethane dyes, are remarkably effective against fungal infections and parasitosis in fish and has been used worldwide as biocide and fungicide in aquaculture since 1930 [1–3]. Efforts have been made to reduce the use of both CV and MG due to their links to genotoxicity, carcinogenicity and other toxic effects [4, 5]. Although the use of these dyes is controlled by guidelines in many regions and countries, CV and MG are still used illegally in some parts of the world due to their low cost and high efficiency, resulting in the frequent occurrence of aquatic products with safety issues [6]. Thus, it is very important to develop efficient methods for the preconcentration of MG and CV in water and seafood regarding the health risks associated with the use of MG and CV.

Many methods, such as liquid chromatography-tandem mass spectrometry [7], high-performance liquid chromatography [8], chemiluminescence [9] and capillary electrophoresis [10] have been proposed for the detection of MG and CV. Expensive instruments or complicated sample preparation processes are required, although these methods are sensitive. Thus, efforts have been devoted to designing suitable and environmentally friendly methods for the preconcentration of MG and CV. Unlike the above techniques, adsorption offers a promising approach for simple, low-cost and rapid preconcentration of MG and CV in environmental samples [11–13].

The development of nanomaterial-based adsorbents has attracted considerable attention due to their rapid, sensitive and high-performance properties. In recent years graphene has become a hot topic of research due to its unique structure and electronic properties [14]. The characteristics of graphene, such as the huge specific surface area [15], graphitised basal plane structure which endows it with strong π - π interactions with the aromatic moieties present in many dyes and facile surface modification [16] make it a promising candidate as high-performance adsorbents. However, problems, such as irreversible aggregation, difficulty in complete collection and its polydispersion [17] limited its application.

Magnetic nanoparticles, as one kind of new nanostructured materials, have attracted increasing attention [18–22] and have been considered as an effective technique for separating magnetic particles from the solution. Compared with traditional adsorbents, magnetic materials have the advantages of avoiding the need of additional centrifugation or filtration which makes the separation easier and faster, or

decreasing the possibility of serious agglomeration and restacking of the graphene sheets which consequently provide a higher available surface area and the enhancement of adsorption capacity owing to the spacing effect of the magnetite nanoparticles between the neighbouring graphene sheets. Fe₃O₄ magnetic nanoparticles, as one of the famous magnetic materials that possess ferromagnetic and supermagnetic properties, are widely used as magnetic carriers for magnetic separation in waste water treatment and as reusable adsorbents in the field of environmental and material sciences, such as the adsorption of carbamate pesticides [23] and dye pollutants [24].

In the work reported in this Letter, graphene/silica magnetic nanocomposites (G/SMNPs) were synthesised and introduced as new and reusable adsorbents for rapid and high-efficiency preconcentration trace amounts of dye pollutants in marine products (Fig. 1). These synthetic adsorbents are non-toxic, common and of low cost. The strength of magnetism and the adsorption effect of the nanocomposites can be conveniently controlled by regulating the ratio of GO and SMNPs which has not been reported so far. In addition, the adsorbents can be easily and quickly separated and enriched from aqueous solutions with the help of an external magnetic field (Fig. 1). The successful preconcentration of typical dye pollutants CV and MG from water samples verified its practicability as dye pollutant adsorbents.

2. Experimental

2.1. Materials and reagents: NaOH, sodium citrate, ethanol, dimethylformamide (DMF) and Na₂CO₃ were purchased from the Bodi Chemical Holding Co. Ltd (Tianjin, China). Tetraethylorthosilicate, 3-(aminopropyl) triethoxysilane and N,N'-dicyclohexylcarbodiimide (DCC) were purchased from the Aladdin Chemical Co. Ltd (Shanghai, China). Graphite power, KMnO₄, FeCl₂·4H₂O, FeCl₃·6H₂O, hydrazine hydrate and NH₃·H₂O was purchased from Asbury Carbons Ltd (Shanghai, China), Jiaozuo Chemical Plant (Henan, China), Kermel Chemical Co. Ltd (Tianjin, China), Tianli Chemical Co. Ltd (Tianjin, China), Sinopharm Chemical Reagent Co. Ltd (Shanghai, China) and Xilong Chemical Co. Ltd (Shantou, China), respectively. All reagents used were of analytical grade. All solutions were freshly prepared before use, and Milli-Q water (18 M Ω cm) was used throughout the experiments.

2.2. Preparation of graphene oxide (GO): GO was synthesised from graphite via a modified Hummers and Offeman's method [25–27].

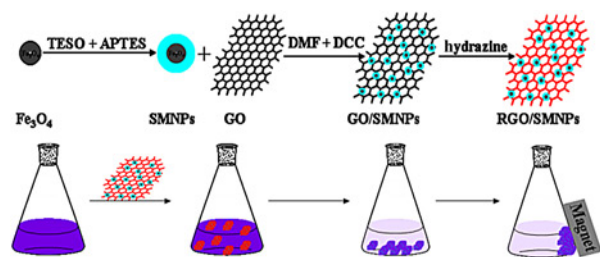


Figure 1 Synthesis and adsorption process of G/SMNPs

Typically, 1.0 g of powdered flake graphite and 0.5 g of NaNO_3 were placed in a 500 mL round bottom flask, followed by the addition of 3 mL of concentrated H_2SO_4 . Then, 3.0 g of KMnO_4 was added slowly to the mixture in an ice bath, to avoid rapid heat evaluation. After 2 h the reaction mixture was stirred at 35°C for 30 min. Finally, the reaction mixture was added to 50 mL of water stirred at 98°C for 30 min, which resulted in the colour change of the mixture from yellow to brown. Then, 85 mL of water was stirred and the reaction was ended with the addition of 4 mL of 30% H_2O_2 . The warm solution was then filtered and subjected to three cycles of precipitation by centrifugation and washed with 5% HCl and then dialysed using a 3000 Da MWCO dialysis bag in deionised water for 48 h. The dry product was dissolved in water ultrasonicated to exfoliate the oxidised graphene.

2.3. Preparation of magnetic (Fe_3O_4): The magnetic nanoparticles were prepared based on the chemical co-precipitation of Fe^{2+} and Fe^{3+} by adding a concentrated base, sodium hydroxide, to the mixture of iron salts in a molar ratio ($\text{FeCl}_2/\text{FeCl}_3$) of 1:2 [28]. Typically, 3.135 g of $\text{FeCl}_2 \cdot 4\text{H}_2\text{O}$ and 8.514 g of $\text{FeCl}_3 \cdot 6\text{H}_2\text{O}$ were added into 100 mL of deionised water. After adding 12.7 mL of NaOH (10 M), the reaction mixture was stirred for 1 h at room temperature. The reaction mixture was then heated to 90°C under continuous stirring for another 1 h. About 0.33 mL of nitric acid was subsequently added to the reaction mixture for 0.5 h at 90°C . A measure of 50 mL of trisodium citrate (0.3 M) was then added, and the mixture was stirred for another 0.5 h. The reaction mixture was allowed to cool, and ethanol was added to precipitate the iron oxides from the aqueous solutions. The mixture was purified with a magnet to collect the synthesised Fe_3O_4 nanoparticles, and then removed supernatant. After repeated washing three times, Fe_3O_4 nanoparticles were dried at 80°C .

2.4. Preparation of SMNPs: SMNPs were prepared by the modified Stöber method. The coating of the iron oxide with silica was carried out in ethanol and deionised water in a ratio of 4:1. Typically, 2 mL of iron oxide in deionised water (1.5%) was suspended in 160 mL of ethanol and 40 mL of deionised water, followed by the addition of 5 mL of aqueous ammonia (25%). This suspension was then homogenised by ultrasonic vibration in a water bath for 15 min. Then, 500 μL of tetraethylorthosilicate/3-(aminopropyl) triethoxysilane (10:1) was added dropwise to the mixture under continuous mechanical stirring. After reaction for 12 h, the mixture was washed thoroughly with ethanol and dried at 80°C .

2.5. Preparation of GO/SMNPs: GO was covalently immobilised on silica by coupling the amino groups of aminosilica and the carboxyl groups of GO. The organic-phase synthesis approach was used to prepare the GO/SMNPs. Typically, 40 mg of GO was dispersed in 25 mL of DMF by the aid of ultrasonication, and then 0.25 g of SMNPs and 10 mg of DCC were added. The mixture was stirred at 55°C for 36 h. The solid product was collected and washed with water and ethanol several times to remove the unbound GO, and finally was dried at 80°C .

2.6. Preparation of G/SMNPs: The G/SMNPs were synthesised by the reduction of GO/SMNPs with hydrazine. Typically, 0.2 g of GO/SMNPs and 0.17 mL of hydrazine hydrate (50%) were added in 10 mL of water. The mixture was kept at 95°C for 2 h. Then, the solid was collected and washed with water and ethanol. Finally, the product was dried at 80°C .

2.7. Apparatus: The crystalline structure and composition of the GO were identified by a D/max-IIIIC X-ray diffractometer (Shimadzu, Japan). Fourier transform infrared (FTIR) spectra were taken with a spectrum one FTIR spectrophotometer (Perkin-Elmer, USA) at room temperature. Atomic force microscopy (AFM) images were collected in the tapping mode using a Nanoscope IIIa. The UV-vis absorption measurements were performed on a Lambda 35 UV analyser (Perkin-Elmer, USA). The fluorescence intensity was recorded on an LS55 fluorescence spectrometer (Perkin-Elmer, USA). The TEM images of the prepared samples were examined using a TecnaiG20 transmission electron microscope (FEL, USA).

3. Results and discussion: characterisation of GO, Fe_3O_4 , SMNPs and G/SMNPs: GO was synthesised from graphite via a modified Hummers and Offeman's method. The synthesised GO was characterised by AFM, X-ray diffraction (XRD) and FTIR spectroscopy (Fig. 2). These characteristics showed that GO sheets with an average thickness of about 1.0 nm were successfully synthesised. XRD data of natural flake graphite and GO are shown in Fig. 2c. Compared with the peak obtained in the diffraction angle 2θ of 26.52° of natural flake graphite which showed its high crystallisation, the diffraction angle 2θ of GO was shown at 10.94° which demonstrated the successful synthesis of GO. The FTIR spectrum of GO further proved the successful synthesis of GO. As shown in Fig. 2d, the FTIR spectrum showed the characteristic vibrations of GO, as reported in a previous work [29], including a broad and intense peak of the O—H group at 3439 cm^{-1} , a C=O peak at 1725 cm^{-1} , an O—H deformation peak at 1394 cm^{-1} , a C—OH stretching peak at 1261 cm^{-1} , an C—O stretching peak at 1060 cm^{-1} and a peak attributed to the vibrations of unoxidised graphitic skeletal domains and the adsorbed water molecules at 1625 cm^{-1} .

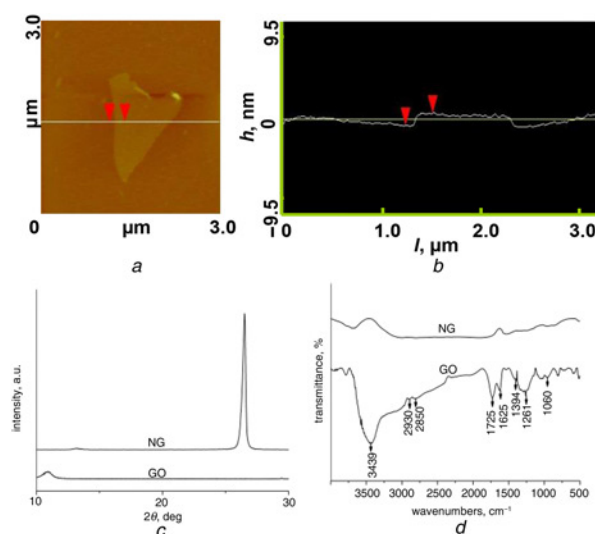


Figure 2 Characterisation of GO
a AFM image
b Height profile of GO
c XRD
d FTIR spectra of GO and natural graphite

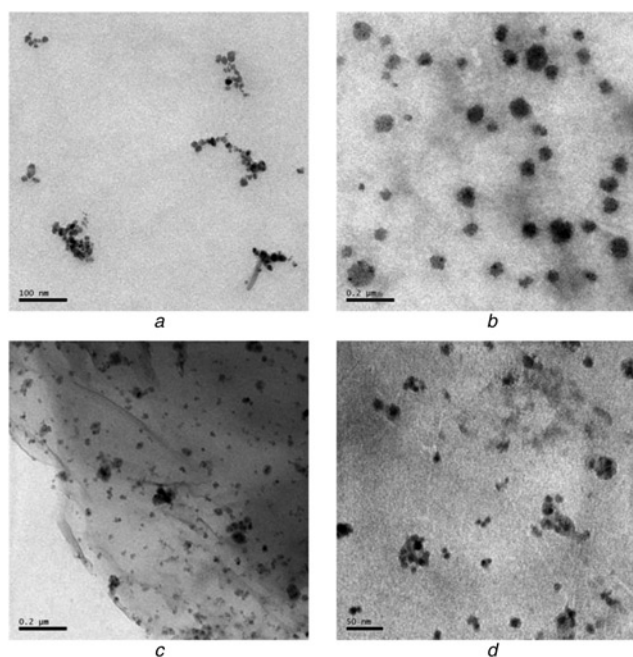


Figure 3 TEM images
a Fe_3O_4
b SMNPs
c, d G/SMNPs

To illustrate the successful synthesis of Fe_3O_4 , SMNPs and G/SMNPs, the synthesised Fe_3O_4 , SMNPs and G/SMNPs were characterised by TEM, XRD and FTIR spectroscopy.

The morphology of the as-prepared Fe_3O_4 , SMNPs and G/SMNPs were investigated by TEM. Particles of Fe_3O_4 can be clearly seen from Fig. 3a. In Fig. 3b, Fe_3O_4 is shown as a small black spot, and the circle of the halo surrounding the small black spot is the silicon layer, which indicated the successful synthesis of SMNPs. G/SMNPs can be clearly observed in Figs. 3c and d. In Fig. 3c, SMNPs are homogeneously dispersed on the graphene sheets. Due to the background of graphene, G/SMNPs can be better observed under high magnification (Fig. 3d). The TEM of Fe_3O_4 , SMNPs and G/SMNPs indicated that Fe_3O_4 , SMNPs and G/SMNPs have been successfully synthesised.

The structural information of G/SMNPs was investigated by XRD. As shown in Fig. 4a, the main diffraction peaks in the 2θ range of 30° – 70° of G/SMNPs correspond to the (50), (50), (75), (50) and (37) five lattice planes of Fe_3O_4 which was consistent with JCPDS Card No. 19–0629 and the diffraction peak at $2\theta = 26.44^\circ$ originated from graphene. FTIR spectra were also measured to characterise the GO and G/SMNPs (Fig. 4b). The FTIR spectrum

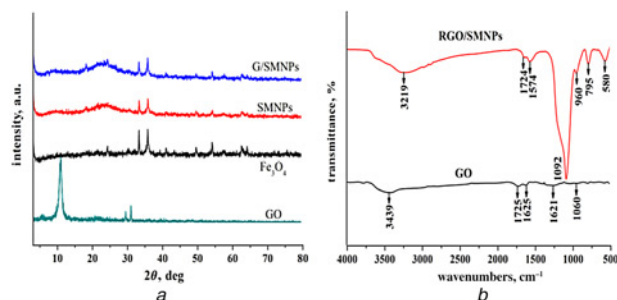


Figure 4 XRD of GO, Fe_3O_4 , SMNPs and G/SMNPs, and FTIR spectra of GO and G/SMNPs
a XRD
b FTIR spectra

of G/SMNPs was significantly different from that of GO. There was a dramatic decrease in the intensities of the characteristic absorption bands of oxygen-related functional groups ($\nu \text{ O-H}$, $\nu \text{ C=O}$ and $\nu \text{ C-O}$). This further suggested the successful reduction of GO to graphene sheets, which was consistent with the XRD results. Furthermore, the typical additional vibrational bands located at 1092 cm^{-1} can be assigned to the giant magnetostrictive vibration of Si–O, confirming the successful synthesis of G/SMNPs.

3.1. Optimisation of the adsorption conditions: To select the optimum adsorption conditions for the extraction of methyl violet and MG, we discuss the effect of pH, adsorption time and the concentration on adsorption.

The pH of the sample solution played an important role in the adsorption of the analytes to the sorbents by both affecting the existing forms of the analytes and their charge species and density on the sorbents surface. The influence of the sample pH on the extraction efficiency of methyl violet and MG was studied over the pH range from 1.5 to 14, 1.5 to 10.77, respectively. The experimental results show that the extraction efficiency had significant changes for methyl violet and MG. The extraction efficiency of methyl violet maintained irregular changes from pH 1.5 to 9, then gradually increased from 9 to 11.54 and finally plummeted from 11.54 to 14 (Fig. 5a). Generally, the optimum pH of the solution is from 10.08 to 11.54, so we chose 10.77 as the optimum pH for methyl violet in this experiment. The extraction efficiency of MG gradually increased from pH 2.5 to 6.47 and then plummeted from 6.47 to 10.77 (Fig. 5b). The reason for this could be that G/SMNPs are not easily destroyed under alkaline conditions. Generally, 10.77 was chosen as the optimum pH for MG in this experiment.

We also tested the effect of adsorption time on the adsorption effect of methyl violet and MG. As shown in Fig. 6a, there was no need to take into account the effect of adsorption time on the adsorption of methyl violet, because the adsorption is a transient absorption. Therefore, we chose 30 min as the optimum adsorption time for methyl violet in this experiment. The removal of MG at

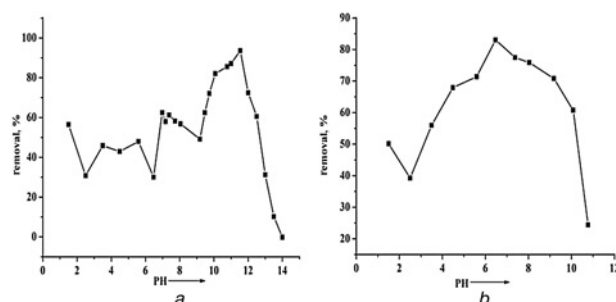


Figure 5 Removal of methyl violet and MG at different pHs
a Methyl violet
b MG

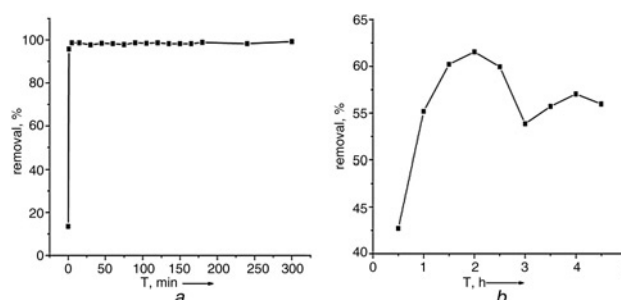


Figure 6 Removal of methyl violet and MG at different times
a Methyl violet
b MG

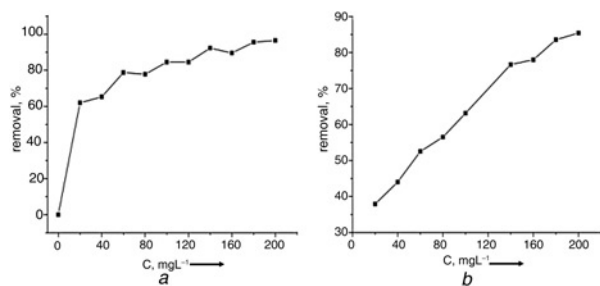


Figure 7 Removal of methyl violet and MG with different concentrations of G/SMNPs
a Methyl violet
b MG

different times had a significant change. As shown in Fig. 6b, 2 h was chosen as the optimum time for MG in this experiment.

To choose the optimum amount of the adsorbent (G/SMNPs) for the extraction of methyl violet and MG, different concentrations of G/SMNPs were tested in the range from 0 to 200 mg L⁻¹. As shown in Fig. 7a, the maximum extraction efficiency of methyl violet was obtained at 140–200 mg L⁻¹ of G/SMNPs and when the amount of adsorbents was above 140 mg L⁻¹, the recoveries remained almost invariant. Thus, 160 mg L⁻¹ G/SMNPs was selected as the optimum amount of adsorbent for methyl violet. Fig. 7b shows that the maximum extraction efficiency of MG was obtained at 140–200 mg L⁻¹ of G/SMNPs and when the amount of adsorbents was above 160 mg L⁻¹, the recoveries remained almost invariant. Therefore, 180 mg L⁻¹ G/SMNPs was selected as the optimum amount of adsorbent for MG.

3.2. Adsorption isotherms: To provide information about the adsorption mechanisms, surface properties and affinity of an adsorbent towards an adsorbate [30], we studied the adsorption isotherm. The adsorption isotherm of methyl violet with different initial concentrations was studied at pH 10.77, with an adsorption time of 15 min, and temperature of 25°C. The adsorption isotherm of MG with different initial concentrations was studied at a pH of 6.47, with an adsorption time of 2 h and at a temperature of 25°C. The adsorption data were analysed according to the well-known Langmuir isotherm models [31]. The Langmuir model assumes uniform energies of adsorption on the surface and no transmigration of the adsorbate in the plane of the surface. It can be expressed as

$$C_e/q_e = C_e/q_m + 1/(K_L q_m) \quad (1)$$

$$q_e = 408.03 (C_0 - C_e)/q_m \quad (2)$$

where q_e is the amount of the adsorbate adsorbed per unit weight of adsorbent (mg g⁻¹), C_0 is the initial concentration of the adsorbate (mg L⁻¹), C_e is the equilibrium concentration of the adsorbate (mg L⁻¹) and q_m and K_L are Langmuir constants related to the maximum adsorption capacity (mg g⁻¹) and energy of adsorption (L mg⁻¹), respectively.

The experimental results show that the adsorption data could be fitted with Langmuir isotherms. Fig. 8 shows the results of data processing and linear fitting. The characteristic parameters of the Langmuir isotherm and linear dependence are shown in Table 1.

3.3. Regeneration and reuse of G/SMNPs: To avoid environmental pollution and meet the need of stringent ecological and economic demands for sustainability, the regeneration and reuse of G/SMNPs is particularly important. To illustrate that the adsorbent G/SMNPs did not only possess high adsorption capability, but also have good desorption properties, we conducted the following

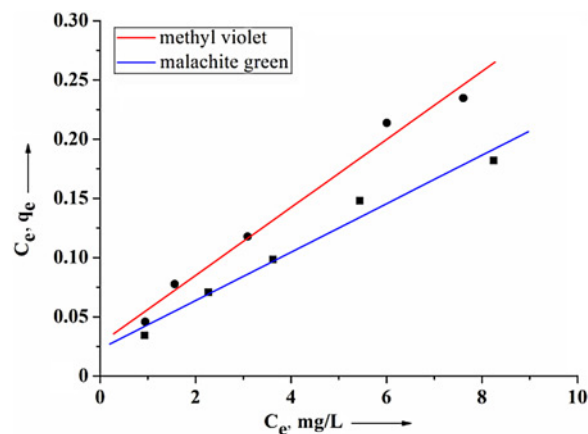


Figure 8 Langmuir linear fitting of methyl violet and MG

Table 1 Linear regression equations and characteristic parameters of methyl violet and MG

Isotherm type	Isotherm constants	Methyl violet	MG
Langmuir	q_m , mg g ⁻¹	34.82	48.90
	K_L , L mg ⁻¹	1.04	0.90
	R^2	0.99	0.99

experiment. The experimental results show that G/SMNPs can be subjected to multiple rounds of reuse by using an inexpensive solvent ethylene glycol as a solution medium. Fig. 9 shows that the removal efficiency of dyes was still more than 80% after reuse in five cycles, indicating that the as-prepared adsorbent had good reusability.

3.4. Applications of G/SMNPs: To evaluate whether the new adsorbent developed here was suitable for practical applications, real water samples, including tap water, Huang Bailing water and lake water collected from Lake Sand in China, were treated using the as-prepared G/SMNPs. The experiments were conducted by adding 10 μM of dyes to the real water samples and then investigating the removal efficiency by adding 0.2 g L⁻¹ of G/SMNPs. The results show that these real water samples had little interference with the performance of G/SMNPs, suggesting that this new adsorbent was suitable for the removal of dyes from real water (Fig. 10). In addition, G/SMNPs also showed excellent

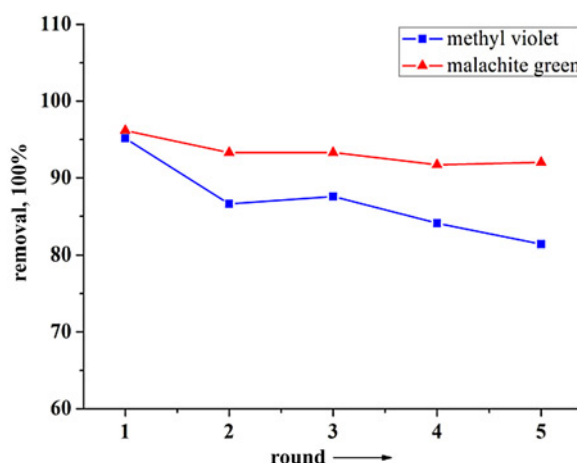


Figure 9 Recycling of G/SMNPs in the removal of dyes (the initial concentration of dye solutions was 10 μM and that of G/SMNPs was 0.6 g L⁻¹)

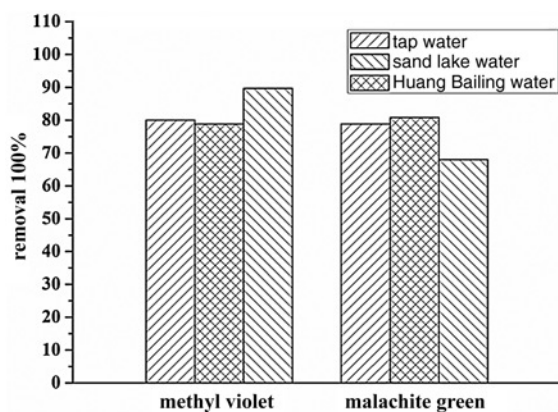


Figure 10 Removal efficiency of dyes in different water samples (the initial concentration of dye solutions and G/SMNPs was $10\ \mu\text{M}$ and $0.2\ \text{g L}^{-1}$, respectively)

removal efficiency for other dye pollutants, including Rhodamine B and methylene blue in industrial wastewater, suggesting that the as-proposed method can be widely used for the removal of dye pollutants in marine environments.

4. Conclusion: Rapid, versatile and high-performance adsorbents were developed for the removal of dye pollutants from water samples. The use of magnetic nanocomposites G/SMNPs endowed the method with easy separation of the adsorbent from the sample solution, high extraction capacity, while taking up less time, and increased absorption efficiency. The exceptional adsorption effect of G/SMNPs demonstrated its practicability as rapid, versatile and high-performance adsorbents for the fast, safe monitoring of marine products.

5. Acknowledgments: This work was financially supported by the Scientific Research Foundation of the Education Commission of Hubei Province (Q20111010 and T201101), the Natural Science Foundation of Hubei Province (2011CDB059 and 2011CDA111) and by the Research Fund for the Doctoral Program of Higher Education of China (20114208120006).

6 References

- [1] Srivastava S., Sinha R., Roy D.: 'Toxicological effects of malachite green', *Aquat. Toxicol.*, 2004, **66**, pp. 319–329
- [2] Afkhami A., Moosavi R., Madrakian T.: 'Preconcentration and spectrophotometric determination of low concentrations of malachite green and leuco-malachite green in water samples by high performance solid phase extraction using maghemite nanoparticles', *Talanta*, 2010, **82**, pp. 785–789
- [3] Long C., Mai Z., Yang Y., *ET AL.*: 'Determination of multi-residue for malachite green, gentian violet and their metabolites in aquatic products by high-performance liquid chromatography coupled with molecularly imprinted solid-phase extraction', *J. Chromatogr.*, 2009, **1216**, pp. 2275–2281
- [4] Littlefield N.A., Blackwell B.N., Hewitt C.C., Gaylor D.W.: 'A novel surface-enhanced Raman scattering sensor to detect prohibited colorants in food by graphene/silver nanocomposite', *Fundam. Appl. Toxicol.*, 1985, **5**, pp. 902–912
- [5] Safarik I., Safarikova M.: 'Detection of low concentrations of malachite green and crystal violet in water', *Water Res.*, 2002, **36**, pp. 196–200
- [6] Stamatii A., Nebbia C., Angelis I.de *ET AL.*: 'Effects of malachite green (MG) and its major metabolite, leucomalachite green (LMG), in two human cell lines', *Toxicol. In Vitro*, 2005, **19**, pp. 853–858
- [7] Abro K., Mahesar S.A., Iqbal S., Perveen S.: 'Quantification of malachite green in fish feed utilizing liquid chromatography-tandem mass spectrometry with a monolithic column', *Food Addit. Contam. A, Chem. Anal Control Expo. Risk Assess.*, 2014, **31**, pp. 827–832
- [8] Kasuga Y., Hishida M., Tanahashi N.: 'Simultaneous determination of malachite green and methylene blue in cultured fish by high-

performance liquid chromatography', *Shokuhin Eiseigaku Zasshi*, 1991, **32**, pp. 137–141

- [9] Zhang Y., Yang J.Y., Lei H.T., *ET AL.*: 'Development of chemiluminescent enzyme immunoassay for the determination of malachite green in seafood', *Food Agr. Immunol.*, 2015, **26**, pp. 204–217
- [10] Sun H.W., Qi H.J.: 'Capillary electrophoresis combined with accelerated solvent extraction as an improved methodology for effective separation and simultaneous determination of malachite green, crystal violet and their leuco-metabolites in aquatic products', *Anal. Methods*, 2013, **5**, pp. 267–272
- [11] Ilayaraja M., Pandi S.M., Meenakshi C., Kannan R.S.: '*Coscinium fenestratum* as a novel adsorbent for the removal of malachite green dye from aqueous solution', *Int. J. Chem. Pharm. Res.*, 2013, **2**, pp. 351–370
- [12] Wang X.S., Zhou Y., Jiang Yu.: 'Evaluation of marine brown *Laminaria japonica* algae as a low-cost adsorbent for the removal of malachite green dye from aqueous solution', *Adsorpt. Sci. Technol.*, 2009, **27**, pp. 537–547
- [13] Etim U.J., Inam E., Umoren S.A., Eduok U.M.: 'Dye removal from aqueous solution using coconut coir dust extract-modified polyvinyl alcohol: a novel adsorbent', *Int. J. Environ. Bioenergy*, 2013, **5**, pp. 62–79
- [14] Bolotin K.I., Sikes K.J., Jiang Z., *ET AL.*: 'Ultrahigh electron mobility in suspended graphene', *Solid State Commun.*, 2008, **146**, pp. 351–355
- [15] Stoller M.D., Park S., Zhu Y., An J., Ruoff R.S.: 'Graphene-based ultracapacitors', *Nano Lett.*, 2008, **8**, pp. 3498–3502
- [16] Zuo X.L., He S.J., Li D., *ET AL.*: 'Graphene oxide-facilitated electron transfer of metalloproteins at electrode surfaces', *Langmuir*, 2010, **26**, pp. 1936–1939
- [17] Green A.A., Hersam M.C.: 'Emerging methods for producing monodisperse graphene dispersions', *J. Phys. Chem. Lett.*, 2010, **1**, pp. 544–549
- [18] Kline T.L., Xu Y.H., Jing Y., Wang J.P.: 'Biocompatible high-moment FeCo-Au magnetic nanoparticles for magnetic hyperthermia treatment optimization', *J. Magn. Magn. Mater.*, 2009, **321**, pp. 1525–1528
- [19] Zhang J.L., Tan X.C., Zhao D.D., *ET AL.*: 'Fe₃O₄ magnetic nanoparticles modified electrode as a sensor for determination of nimesulide', *Chem. Res. Chin. Univ.*, 2011, **27**, pp. 566–569
- [20] Wu Y., Wang Y.J., Luo G.S., Dai Y.Y.: 'In situ preparation of magnetic Fe₃O₄-chitosan nanoparticles for lipase immobilization by cross-linking and oxidation in aqueous solution', *Bioresour. Technol.*, 2009, **100**, pp. 3459–3464
- [21] Cheng G.F., Huang C.H., Zhao J., Tan X.L., He P.G., Fang Y.Z.: 'A novel electrochemical biosensor for deoxyribonucleic acid detection based on magnetite nanoparticles', *Chin. J. Anal. Chem.*, 2009, **37**, pp. 169–173
- [22] Guo S.J., Li D., Zhang L.X., Li J., Wang E.K.: 'Monodisperse mesoporous superparamagnetic single-crystal magnetite nanoparticles for drug delivery', *Biomaterials*, 2009, **30**, pp. 1881–1889
- [23] Wu Q.H., Zhao G.Y., Feng C., Wang C., Wang Z.: 'Preparation of a graphene-based magnetic nanocomposite for the extraction of carbamate pesticides from environmental water samples', *J. Chromatogr. A*, 2011, **1218**, pp. 7936–7942
- [24] Sun H.M., Cao L.Y., Lu L.H.: 'Magnetite/reduced graphene oxide nanocomposites: one step solvothermal synthesis and use as a novel platform for removal of dye pollutants', *Nano Res.*, 2011, **4**, pp. 550–562
- [25] Hummers W.S., Offeman R.E.: 'Preparation of graphitic oxide', *J. Am. Chem. Soc.*, 1958, **80**, p. 1339
- [26] Stankovich S., Piner R.D., Chen X.Q., Wu N.Q., Nguyen S.T., Ruoff R.S.: 'Stable aqueous dispersions of graphitic nanoplatelets via the reduction of exfoliated graphite oxide in the presence of poly(sodium 4-styrenesulfonate)', *J. Mater. Chem.*, 2006, **16**, pp. 155–158
- [27] Gilje S., Han S., Wang M.S., Wang K.L., Kaner R.B.: 'A chemical route to graphene for device applications', *Nano Lett.*, 2007, **7**, pp. 3394–3398
- [28] Yang Y.M., Aw J., Chen K., *ET AL.*: 'Enzyme-responsive multifunctional magnetic nanoparticles for tumor intracellular drug delivery and imaging', *Chem. Asian J.*, 2011, **6**, pp. 1381–1389
- [29] Xu Y.X., Bai H., Lu G.W., Li C., Shi G.Q.: 'Flexible graphene films via the filtration of water-soluble noncovalent functionalized graphene sheets', *J. Am. Chem. Soc.*, 2008, **130**, pp. 5856–5857
- [30] Vijayakumar G., Yoo C.K., Elango K.G.P., Dharmendrakumar M.: 'Adsorption characteristics of Rhodamine B from aqueous solution onto baryte', *CLEAN*, 2010, **38**, pp. 202–209
- [31] Langmuir I.: 'The adsorption of gases on plane surfaces of glass, mica and platinum', *J. Am. Chem. Soc.*, 1918, **40**, pp. 1361–1402